photonics

MDPI

Article

Beam Properties of a Partially Coherent Beam Propagating Horizontally in Atmospheric Turbulence

Zengyan Wu *, Zhejun Feng, Shubing Ye, Baoming Song, Runxi Wei and Chaoran Yu

School of Optoelectronic Engineering, Xidian University, Xi'an 710071, China; zhjfeng@mail.xidian.edu.cn (Z.F.); sbye@stu.xidian.edu.cn (S.Y.)

* Correspondence: zywu_21@stu.xidian.edu.cn

Abstract: This study explored the impact of atmospheric turbulence on partially coherent light propagation. Atmospheric turbulence causes random modulation of the intensity and phase of light, resulting in a speckle pattern in the far field. This study focused on partially coherent Gaussian Schell model beams and derived an analytical expression of the cross-spectral density function for their transmission through atmospheric turbulence, based on the generalized Huygens–Fresnel principle and the Tatarski spectrum model. Numerical simulations were used to investigate the effects of the source parameters and turbulence strength on the intensity distribution, beam width, and coherence length of partially coherent light in horizontal atmospheric transmission. The results demonstrate that diffraction-induced broadening primarily affects the intensity distribution of light in free-space transmission. Short transmission distances in atmospheric turbulence have comparable characteristics to those in a vacuum; however, as the turbulence intensity and transmission distance increase, the beam broadening effect amplifies, and the coherence length is reduced. The findings are relevant to the design of acquisition, pointing, and tracking systems for wireless laser communication systems and offer insights into the optimization of optical systems for atmospheric conditions.

Keywords: atmospheric turbulence; partially coherent; speckle effect; coherence length

Citation: Wu, Z.; Feng, Z.; Ye, S.; Song, B.; Wei, R.; Yu, C. Beam Properties of a Partially Coherent Beam Propagating Horizontally in Atmospheric Turbulence. *Photonics* **2023**, *10*, 477. https://doi.org/10.3390/photonics10040477

Received: 27 March 2023
Revised: 17 April 2023
Accepted: 19 April 2023
Published: 21 April 2023

1. Introduction

During their propagation through the atmosphere, light waves experience a range of interactions, including absorption, scattering, and random phase fluctuations. The primary drivers of the absorption and scattering effects are atmospheric molecules, suspended particles, and aerosols, resulting in the attenuation of light wave energy along its transmission path. The intensity of these effects is contingent upon the wavelength of the light wave in question. Meanwhile, atmospheric turbulence denotes the irregular and stochastic movement of air in the atmosphere, giving rise to fluctuations in physical parameters such as pressure, velocity, and temperature at individual points within the system [1–3]. This turbulence belongs to the category of weak scattering media; hence, the backscattering effect of light beams and the polarization degradation (coupling) effects can be considered negligible. Laser beams are highly directional but vulnerable to their propagation medium, especially atmospheric turbulence; this results in refractive index fluctuations, causing random drifting, beam jitters, and intensity fluctuations [4–6]. The impact of atmospheric turbulence on laser beams is a critical concern for various applications, such as remote sensing, tracking, and long-range optical communications, including the design of the APT system in wireless laser communication systems [7]. For a considerable period, the impact of atmospheric turbulence on free-space optical communication [8,9], laser radar, and laser imaging has been a matter of great concern [10–12]. Research on partially coherent light sources has increased due to the proven fact that highly directional laser beams do not necessarily have high spatial coherence [13]. Partially coherent light propagates when coherent light passes through a medium affected by turbulence, and laser beams often

emit partially coherent multimodal beams in the form of Gaussian Schell model beams. Therefore, it is necessary to conduct a comprehensive investigation on the variations in the properties of partially coherent light beams under the influence of atmospheric turbulence.

Until now, investigations on partially coherent light have primarily focused on the beam divergence angle, scintillation effects, intensity distribution, and spatial coherence under atmospheric turbulence conditions. For instance, Eyyuboglu et al. delved into the spatial coherence properties of partially coherent light under atmospheric turbulence [14]. Richlin et al. previously investigated the scintillation and aperture smoothing factor of partially coherent light under similar conditions, utilizing the cross-spectral density function [15]. The present research, carried out by Greg Gbur and his colleagues, offers an analysis of the impact of the medium on partially coherent beams, and identifies the specific conditions under which these beams are less affected and the extent to which this occurs. The primary focus of the study is on the broadening of partially coherent beams in the presence of turbulence. It should be noted, however, that the investigation solely examines the variation law of the effective width with the propagation distance [16], but it does not encompass the broader scope of beam broadening under other influencing factors. Therefore, further research in this area is required to better understand the behavior of partially coherent beams in diverse scenarios. Xing et al. conducted a theoretical investigation of the scattering behavior of Gaussian Schell beams in a turbulent atmosphere interacting with diffuse targets to explore the effects of atmospheric turbulence on the scattering characteristics of partially coherent light beams [17]. While this study provides insights into the scattering properties of such beams in atmospheric turbulence, it fails to address the effects of atmospheric turbulence on laser transmission, such as the effective width of the beam and light intensity flicker, which can significantly impact the detection accuracy of the spot centroid of the APT system. Therefore, a detailed theoretical analysis of beam width characteristics induced by atmospheric turbulence is necessary to provide a theoretical reference for the design of space optical communication systems. In a previous study, Friberg conducted an analysis of the beam width and wavefront curvature radius characteristics of partially coherent light in free space and investigated their spatial coherence properties [18]. However, the analysis solely focused on the vacuum transmission of light beams. Considering the practical application requirements, it is imperative to conduct further investigations on the transmission of partially coherent light in turbulent flows. The spatial coherence and polarization properties of laser beams can be elucidated by examining changes in the transverse coherence length. A new model, the multi-Gaussian Schell model (MGSM) beam, was introduced as a means of characterizing the spectral coherence of laser beams using a multi-Gaussian distribution [19,20]. The beam conditions of the MGSM beam were obtained, and it has been demonstrated that the MGSM beam model provides a flexible means of characterizing laser beams with varying degrees of coherence. In a prior study, REN [21] conducted numerical simulations to investigate the changes in the light intensity distribution and coherence length of fully and partially coherent light under different turbulence intensities. However, to accurately study the impact of atmospheric turbulence on coherence length, it is essential to exclude the influence of light source extension. In this paper, we highlight the inadequacy of analyzing atmospheric turbulence solely through the change in the transverse coherence length; we also propose the analytical use of the ratio of coherence length to beam width. Despite the existing research on the coherence and light intensity characteristics of partially coherent light in atmospheric turbulence, the coherence characteristics of beams with different light source coherence parameters require further research and analysis. As theoretical models continue to advance and the demand for practical applications increases, it is necessary to further analyze the transmission characteristics of partially coherent light in atmospheric turbulence.

The present study focuses on the Gaussian Schell model (GSM) beam as a partial coherence model and aims to derive the analytical expression of the cross-spectral density function for the transmission of GSM beams in the horizontal atmospheric channel, based

on the generalized Huygens–Fresnel principle. The obtained expression is then used to conduct numerical simulations and a theoretical analysis of the intensity distribution and coherence length changes in both fully and partially coherent light under different turbulence strengths and coherence parameters. Based on these considerations, we investigated the individual impacts of source beam parameters such as the waist radius, transverse coherence length, and wavelength on both the effective beam width and effective coherence length of the received beam. An isolated examination of atmospheric turbulence effects through coherence length analysis falls short in accounting for beam spreading effects. As such, the ratio of the effective coherence length to the effective beam width was scrutinized to account for the influence of beam parameters. The study investigates the transmission of partially coherent light beams and analyzes the effects of atmospheric turbulence on beam propagation. The analysis considers the atmospheric refractive index structure constant and inner scale to evaluate the influence of turbulence intensity on beam transmission. Our study provides a comprehensive analysis of the transmission characteristics of partially coherent light beams, and the results are applicable not only to laser transmission but also to general electromagnetic beam transmission. The findings offer a theoretical reference for designing space optical communication systems.

2. Materials and Methods

2.1. Introduction to Atmospheric Turbulence Properties

Atmospheric turbulence arises due to the erratic motion of air in the atmosphere, resulting in non-uniform fluctuations in air pressure, temperature, and density. The refractive index of the atmosphere is contingent upon these parameters and therefore exhibits irregular spatial and temporal changes. The impact of turbulent flow on light waves manifests primarily in the form of fluctuations in the light intensity (flickering), phase (spatial and temporal), and direction (beam drift), among other phenomena. In addition to the absorption and scattering of optical signals by atmospheric gas molecules, the random fluctuations in the refractive index induced by atmospheric turbulence must also be taken into account. The passage of an optical signal through the atmospheric channel results in the occurrence of various phenomena, such as fluctuations in the light intensity and arrival angle, as well as beam drift, expansion, and wavefront distortion. These factors collectively contribute to the degradation of beam quality, thereby adversely impacting the performance and overall quality of the laser communication system [22,23].

To intuitively observe the influence of turbulence on light, researchers can employ an atmospheric turbulence phase screen to conduct numerical simulations. The process involves placing all phase distortions within the atmosphere onto a square phase screen with a side length of 1 m and 512 × 512 sampling points. The simulation employs an atmospheric structure constant of 2×10^{-15} $m^{-2/3}$, a turbulent layer thickness of 100 m, and a laser wavelength of 1062 nm, and the fifth harmonic is added for compensation. Figure 1 displays the resulting phase screen, which reveals the significant phase distortion caused by turbulence. Consequently, there is a need to quantitatively determine the coherence and light intensity characteristics of partially coherent light in atmospheric turbulence and to conduct comprehensive research and analysis.

The current study describes the mathematical extension of the turbulence spectrum used by Tatarski and von Karman to encompass the entire range of spatial frequencies, while concurrently circumventing singularities. As the Tatarski turbulence spectrum function is utilized in the subsequent analysis, it is briefly introduced herein. This function is frequently employed to evaluate the energy distribution of turbulence fields at diverse scales, providing a comprehensive understanding of the behavior and statistical properties of turbulence at various levels. Moreover, Figure 2 presents the relationship between the Tatarski turbulence spectrum function and the wave number.

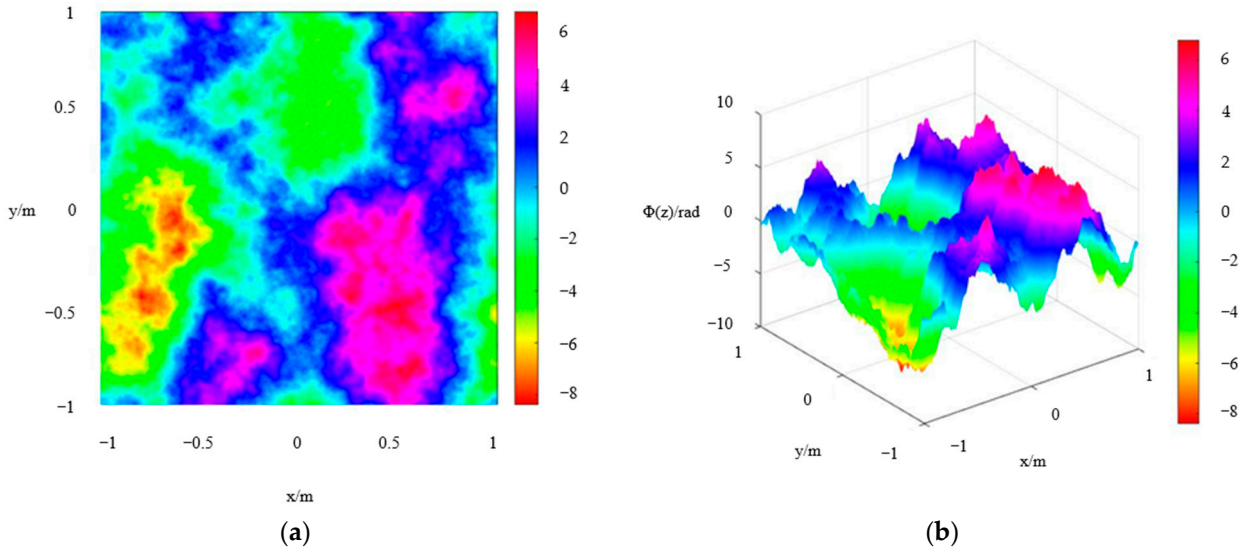

Figure 1. Simulated atmospheric turbulence phase screen. (**a**) Two-dimensional graph; (**b**) Three-dimensional graph.

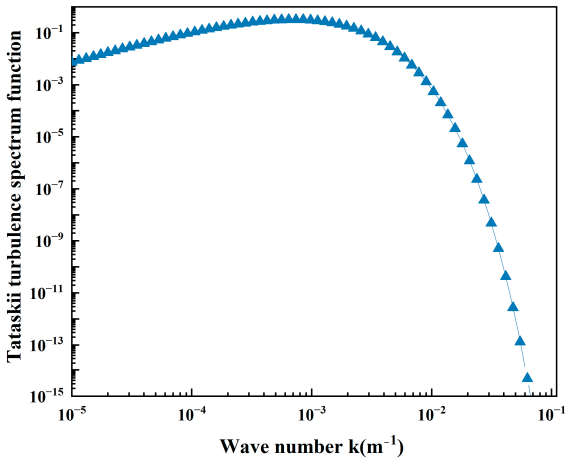

Figure 2. Tatarski turbulence spectral function.

The present analysis indicates that the curve displayed in the graph is relatively flatter when the wavenumber is small, indicating a larger length scale. This phenomenon can be attributed to the strong turbulence generated in the lower layers of the atmosphere due to the combined effects of viscosity and gravity, which result in significant changes in the velocity and pressure of air, leading to the formation of eddies and vortices of various length scales. These eddies and vortices dissipate energy from the turbulent flow, with the turbulent energy mainly being concentrated at larger length scales. On the other hand, as the wave number increases, the curve exhibits an exponential downward trend. This behavior is primarily observed in the upper layers of the atmosphere due to the presence of suspended matter such as dust and water droplets and the cross-layer transmission of photons, all of which limit the propagation and diffusion of turbulent energy. The presence of this suspended matter and photons causes the turbulent energy distribution to become concentrated on smaller length scales. It should be noted that the present analysis is a simplified model, and the actual distribution of turbulent energy can be affected by various atmospheric conditions such as height, gas composition, and turbulence characteristics.

2.2. Theoretical Derivation

The transmission schematic of a partially coherent Gaussian Schell model (GSM) beam through atmospheric turbulence from the z = 0 plane to the z > 0 plane is shown in Figure 3. Here, the GSM surface source occupies a finite domain σ. Assuming that the spectral density of the field passing through the source is represented by $S^{(0)}(\mathbf{r}, \omega)$ and the spectral degree of coherence is represented by $h^{(0)}(\mathbf{r_1}, \mathbf{r_2}, \omega)$, the expressions are given as follows:

$$S^{(0)}(\mathbf{r}, \omega) = I_0 \exp\left(-\frac{|\mathbf{r}|^2}{2\sigma_S^2}\right) \tag{1}$$

$$h^{(0)}(\mathbf{r_1}, \mathbf{r_2}, \omega) = \exp\left(-\frac{|\mathbf{r_1} - \mathbf{r_2}|^2}{2\sigma_h^2}\right) \tag{2}$$

where $\mathbf{r} = (\mathbf{r_1}, \mathbf{r_2})$ is the optical field vector at two different points on the transverse section perpendicular to the direction of light transmission. σ_S represents the waist radius of the source beam and σ_h is the coherence length of the source field, which determine the effective width of the spectral density and spectral coherence of the entire source, respectively. As σ_h increases, the coherence of the beam increases; when it increases to infinity, the source field becomes completely coherent light. The cross-spectral density function (CSDF) of the partially coherent GSM collimated beam at L = 0 can be obtained from Expressions (1) and (2).

$$\begin{aligned} W^{(0)}(\mathbf{r_1}, \mathbf{r_2}, \omega) &= \sqrt{S^{(0)}(\mathbf{r_1}, \omega)}\sqrt{S^{(0)}(\mathbf{r_2}, \omega)} \times h^{(0)}(\mathbf{r_1}, \mathbf{r_2}, \omega) \\ &= I_\Lambda \exp\left(-\frac{\mathbf{r_1}^2 + \mathbf{r_2}^2}{4\sigma_S^2}\right) \times \exp\left(-\frac{(\mathbf{r_1} - \mathbf{r_2})^2}{2\sigma_h^2}\right) \end{aligned} \tag{3}$$

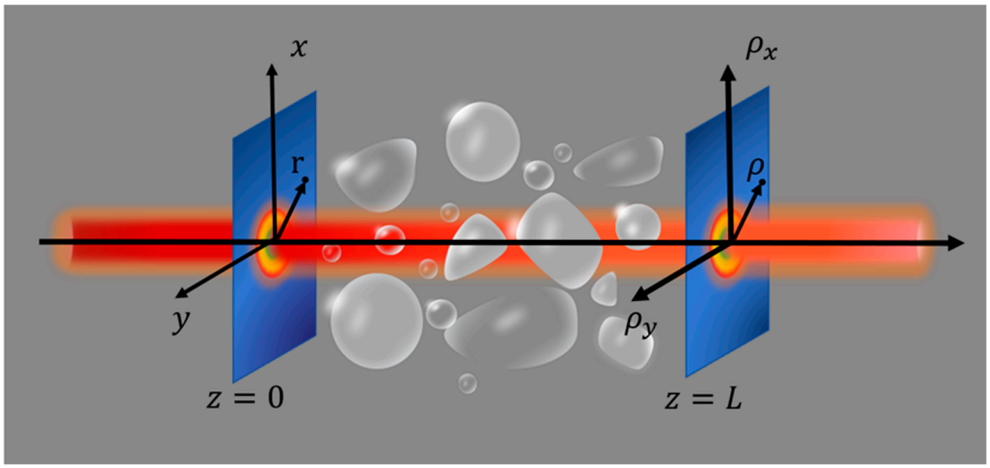

Figure 3. Schematic diagram of the light wave passing through a turbulent atmosphere from the incident surface and reaching the exit surface.

The amplitude of the optical field after the emission of the beam and its propagation through a turbulent medium over a distance of L is:

$$\begin{aligned} U(\boldsymbol{\rho}, L, \omega) &= -\frac{ik\exp(ikL)}{2\pi L}\iint U_0(\boldsymbol{\rho_0}, \omega) \\ &\times \exp\left[ik\frac{(\boldsymbol{\rho} - \boldsymbol{\rho_0})^2}{2L}\right]\exp[\Psi(\boldsymbol{\rho}, \boldsymbol{\rho_0}, L)]d^2\boldsymbol{\rho_0} \end{aligned} \tag{4}$$

where $\boldsymbol{\rho} = (\boldsymbol{\rho}_1, \boldsymbol{\rho}_2)$ is a two-dimensional position vector on the z > 0 plane. U_0 represents the amplitude of the incident field, Ψ represents the random phase function introduced by the turbulent medium properties, $k = \omega/c = 2\pi/\lambda$ is the wave number associated with the frequency ω, and c is the speed of light in a vacuum. In this context, we introduce

the cross-spectral density function, which is a well-established quantitative technique for characterizing the correlation between two distinct signals in the frequency domain. It has extensive applications across diverse domains, including signal processing, communication engineering, and seismology, among others. The computation of cross-spectral density involves Fourier transforming the two signals and then multiplying them to derive the inverse Fourier transform. In the domain of optics, the cross-spectral density function is used to model the interaction and interference between beams. It enables us to analyze various features of optical beams, such as the coherence, phase difference, and optical path difference. According to the Huygens–Fresnel diffraction principle and Formula (4), the cross-spectral density (i.e., intensity at a specific frequency) function at the target location after the far-distance transmission of the GSM partially coherent beam through atmospheric turbulence is defined as [16]:

$$\begin{array}{rcl} I(\boldsymbol{\rho}_1, \boldsymbol{\rho}_2, L) & = & W(\boldsymbol{\rho}_1, \boldsymbol{\rho}_2, \omega) = \langle U^*(\boldsymbol{\rho}_1, L, \omega) U(\boldsymbol{\rho}_2, L, \omega) \rangle_M \\ & = & \left(\frac{1}{\lambda L}\right)^2 \iint \mathrm{d}^2\rho_1 \iint \mathrm{d}^2\rho_2 W^{(0)}(\boldsymbol{\rho_1}, \boldsymbol{\rho_2}, \omega) \\ & \times & \langle \exp[\Psi^*(\rho_1, r_1) + \Psi(\rho_2, r_2)] \rangle_M \\ & \times & \exp\left[\frac{ik}{2L}(r_2 - \rho_2)^2 - (r_1 - \rho_1)^2\right] \end{array} \tag{5}$$

The second-to-last term in the integrated function on the right-hand side of Equation (5) can be expressed by the following expression:

$$\begin{array}{l} \langle \exp[\Psi^*(\boldsymbol{\rho_1}, r_1) + \Psi(\boldsymbol{\rho_2}, r_2)] \rangle_M \\ = \exp\left(\begin{array}{l} -4\pi^2 k^2 L \int_0^1 \int_0^\infty \kappa \Phi_n(\kappa) \\ \cdot \{1 - J_0[|(1-\xi)(\boldsymbol{\rho_1} - \boldsymbol{\rho}_2) + \xi(r_1 - r_2)|\kappa]\} \mathrm{d}\kappa \mathrm{d}\xi \end{array} \right) \\ = \exp\left[-\frac{1}{2} D_{SP}(\boldsymbol{\rho_1} - \boldsymbol{\rho}_2, r_1 - r_2, L)\right] \end{array} \tag{6}$$

where J_0 is the zero-order Bessel function of the first kind, and $\Phi_n(\kappa)$ is the refractive index spectrum function of the turbulent medium. The Tatarski spectrum is used in this article. $\Phi_n(\kappa) = 0.033 C_n^2 \kappa^{-11/3} \exp\left(-\frac{\kappa^2}{\kappa_m^2}\right)$, $\kappa_m = 5.92/l_0$, and $\kappa \geq 1/L_0$. l_0, L_0 represent the inner and outer scales of turbulence, respectively. κ is the spatial wave number, $\boldsymbol{\kappa} = (\kappa_x, \kappa_y)$ is the magnitude of the spatial frequency vector, and $\boldsymbol{\kappa}$ and $\mathbf{r}$ are a Fourier transform pair in spatial coordinates. D_{SP} is the phase structure factor for the transmission of spherical waves in a uniformly isotropic turbulent atmosphere. $\boldsymbol{\rho_1} - \boldsymbol{\rho}_2$ and $r_1 - r_2$ represent the position vector differences on the outgoing and incoming surfaces, respectively. Under the condition of strong turbulence, i.e., when the transverse coherence length of the coherent Gaussian beam propagating in the turbulence is much smaller than the inner scale of the turbulence at a certain propagation distance, J_0 can be approximated by the first two terms of the power series expansion of the zero-order Bessel function of the first kind. Equation (6) can be simplified as:

$$\begin{array}{l} \langle \exp[\Psi^*(\boldsymbol{\rho_1}, r_1) + \Psi(\boldsymbol{\rho_2}, r_2)] \rangle_M \\ = \exp\left(\begin{array}{l} -4\pi^2 k^2 L \int_0^1 \int_0^\infty \kappa \Phi_n(\kappa) \\ \cdot \left\{\frac{1}{4}[|(1-\xi)(\boldsymbol{\rho_1} - \boldsymbol{\rho}_2) + \xi(r_1 - r_2)|\kappa]^2\right\} \mathrm{d}\kappa \mathrm{d}\xi \end{array} \right) \\ \approx \exp\left(-\Gamma\left[n^2 + nu + u^2\right]\right) \end{array} \tag{7}$$

The corresponding parameters are:

$$\begin{array}{c} \Gamma = \frac{1}{3}\pi^2 k^2 L \int_0^\infty \kappa^3 \Phi_n(\kappa) \mathrm{d}\kappa \\ n = \boldsymbol{\rho_1} - \boldsymbol{\rho}_2, u = r_1 - r_2 \end{array}$$

By substituting the final simplified results of Equations (3) and (7) into Equation (5), we obtain:

$$\begin{aligned} I(\boldsymbol{\rho}_1, \boldsymbol{\rho}_2, L) &= W(\boldsymbol{\rho}_1, \boldsymbol{\rho}_2, \omega) \\ &= \left(\tfrac{1}{\lambda L}\right)^2 \iint \mathrm{d}^2\rho_1 \iint \mathrm{d}^2\rho_2 \\ &\times I_\Delta \exp\left(-\tfrac{\boldsymbol{\rho_1}^2+\boldsymbol{\rho_2}^2}{4\sigma_S^2}\right) \times \exp\left(-\tfrac{(\boldsymbol{\rho_1}-\boldsymbol{\rho_2})^2}{2\sigma_h^2}\right) \\ &\times \exp\left(-\Gamma\left[n^2+nu+u^2\right]\right) \\ &\times \exp\left[\tfrac{ik}{2L}(r_2-\rho_2)^2-(r_1-\rho_1)^2\right] \end{aligned} \tag{8}$$

Performing complex integration on the above equation yields the expression for the CSDF of the GSM beam at a propagation distance of L:

$$\begin{aligned} I(\boldsymbol{\rho}_1, \boldsymbol{\rho}_2, L) &= W(\boldsymbol{\rho}_1, \boldsymbol{\rho}_2, \omega) \\ &= \tfrac{I_\Delta \sigma_S^2}{Q(L)} \exp\left(-\tfrac{v^2}{8Q(L)}\right) \times \exp\left(\tfrac{ikuv}{2M(L)}\right) \\ &\times \exp\left[-\left(\Gamma+\tfrac{1}{8\Omega(L)}-\tfrac{P(L)}{8Q(L)}\right)u^2\right] \end{aligned} \tag{9}$$

The corresponding parameters are:

$$m = \boldsymbol{\rho_1} + \boldsymbol{\rho_2}, v = r_1 + r_2$$

$$\gamma_0 = \frac{L}{2k\sigma_S^2}$$

$$\Omega(L) = (\sigma_S \gamma_0)^2$$

$$P(L) = \left(\frac{1}{\gamma_0} - 4\gamma_0\Gamma\sigma_S^2\right)^2$$

$$Q(L) = \sigma_S^2 + \frac{L^2}{4k^2\sigma_S^2} + \frac{L^2}{k^2\sigma_h^2} + \frac{2\Gamma L^2}{k^2}$$

$$M(L) = \frac{LQ(L)}{\sigma_S^2 P(L)^{\frac{1}{2}}\gamma_0 - Q(L)}$$

As noted above, the CSDF represents the intensity at a specific frequency. Therefore, when $\boldsymbol{\rho} = \boldsymbol{\rho_1} = \boldsymbol{\rho_2}$, the optical intensity at the z > 0 plane can be obtained as:

$$\begin{aligned} I(\boldsymbol{\rho}, L) &= W(\boldsymbol{\rho}, \omega) \\ &= \tfrac{I_\Delta \sigma_S^2}{Q(L)} \exp\left(-\tfrac{\boldsymbol{\rho}^2}{2Q(L)}\right) \end{aligned} \tag{10}$$

Generally, the effective width of the beam refers to the beam width when the field amplitude value drops to $1/e$. The beam width μ_σ is defined as [16]:

$$\mu_\sigma(L) = \left(\frac{\int\int_{-\infty}^{+\infty} \boldsymbol{\rho}^2 I(\boldsymbol{\rho}, L) d^2\boldsymbol{\rho}}{\int\int_{-\infty}^{+\infty} I(\boldsymbol{\rho}, L) d^2\boldsymbol{\rho}}\right)^{1/2} \tag{11}$$

Substituting Equation (10) into Equation (11), we obtain:

$$\mu_\sigma(L) = (2Q(L))^{1/2} \tag{12}$$

According to the expression for the GSM beam CSDF for a propagation distance of L (Equation (8)), the complex coherence factor of the beam can be expressed as:

$$\begin{aligned} \varsigma_{DOC} &= \frac{W(\boldsymbol{\rho}_1,\boldsymbol{\rho}_2,\omega)}{W(\boldsymbol{\rho}_1,\boldsymbol{\rho}_1,\omega)^{1/2}W(\boldsymbol{\rho}_2,\boldsymbol{\rho}_2,\omega)^{1/2}} \\ &= \exp\left(\frac{ikuv}{2M(L)}\right) \times \exp\left[-\left(\Gamma + \frac{1}{8\Omega(L)} - \frac{P(L)}{8Q(L)}\right)u^2\right] \end{aligned} \tag{13}$$

Considering the second term in Equation (13) as the amplitude of the beam's complex coherence factor, denoted as $H(u, L)$, then:

$$H(u,L) = \exp\left[-\left(\Gamma + \frac{1}{8\Omega(L)} - \frac{P(L)}{8Q(L)}\right)u^2\right] \tag{14}$$

Similar to Equation (11), we can obtain the effective coherence length as:

$$\mu_\delta(L) = \left(\frac{\int\int_{-\infty}^{+\infty} u^2 H(u,L)d^2u}{\int\int_{-\infty}^{+\infty} H(u,L)d^2u}\right)^{1/2} \tag{15}$$

Substituting Equation (14) into Equation (15), we obtain:

$$\mu_\delta(L) = \left(\Gamma + \frac{1}{8\Omega(L)} - \frac{P(L)}{8Q(L)}\right)^{1/2} \tag{16}$$

Combining Equations (12) and (16), we can comprehensively analyze the characteristics of partially coherent light propagation.

3. Numerical Analysis of Partially Coherent Light Propagation

The present study derives the analytical expression for the cross-spectral density function of a Gaussian Schell model (GSM) beam in propagation via the generalized Huygens–Fresnel principle. The results reveal that the coherence length of the beam is influenced by both the source parameters and turbulence factors during light propagation. Numerical simulations and theoretical analyses were conducted to evaluate the intensity distribution, effective beam width, and coherence length of partially coherent light under varying source parameters and turbulence scales. This simulation experiment adopts the method of controlling variables. When analyzing the impact of a particular variable, if there are no specific instructions, for the sake of convenience, the values of other parameters will be selected from the last column in Table 1 for the calculation.

Table 1. Range of parameter values in the numerical simulation.

Parameters	Symbol	Numerical Value	Reference Value
Wavelength	λ	532~1315 nm	532 nm
Light source scale (waist radius)	σ_S	1~4 cm	3 cm
Light source scale (coherence length)	σ_h	1~4 mm	1 mm
Atmospheric refractive index structure constant	C_n^2	10^{-16} m$^{-2/3}$~5×10^{-14} m$^{-2/3}$	10^{-15} m$^{-2/3}$
Atmospheric inner scale	l_0	10^{-4}~10^{-2} m	5×10^{-3} m

3.1. The Intensity Distribution of Fully Coherent Light and Partially Coherent Light under Different Source Parameters and Transmission Conditions

Figure 4 shows the normalized optical intensity curve at a distance of r = 1 cm from the center as a function of transmission distance for different source coherence levels under different turbulence strengths. The coherence parameter of a laser, denoted as ℓ, $\ell = 1 + 4\sigma_s^2/\sigma_h^2$, is a metric that describes the coherence of its light source. $\ell = 1$ indicates that the light source is an ideal, completely coherent light. However, if ℓ exceeds 1, the light

source becomes partially coherent. It is worth noting that as the coherence parameter of the light source increases, the spatial coherence of the laser tends to decrease. Using fully coherent light ($\ell = 1$), the received optical intensity is normalized after transmitting over a distance of L = 1 km and through atmospheric turbulence with a strength of $C_n^2 = 10^{-16}$. The effect of turbulence on the optical intensity distribution for fully coherent light is presented in Figure 4a, which shows an increase in beam size on the receiving plane and a rapid decrease in normalized optical intensity as the turbulence strength increases. In comparison to fully coherent light, the peak center optical intensity difference is reduced for partially coherent light under varying turbulence strengths, as shown in Figure 4b–d. As the coherence parameter rises, the peak optical intensity values become increasingly similar across different turbulence strengths. When examining the effects of atmospheric turbulence on the received optical intensity, the coherence parameter (source coherence) plays a more significant role under conditions of weak atmospheric turbulence ($C_n^2 = 10^{-16}$), as depicted in Figure 4a–d. Conversely, at greater levels of atmospheric turbulence ($C_n^2 = 5 \times 10^{-14}$), increasing the coherence parameter has a minimal impact on the average optical intensity at the receiving plane. In regions of weak turbulence, the impact of the coherence parameter of the light source on the average received light intensity is more pronounced; as the turbulence strength increases, the effect of the coherence parameter of the light source decreases. In contrast, in regions of strong turbulence, the effect of atmospheric turbulence on the received light intensity becomes more dominant.

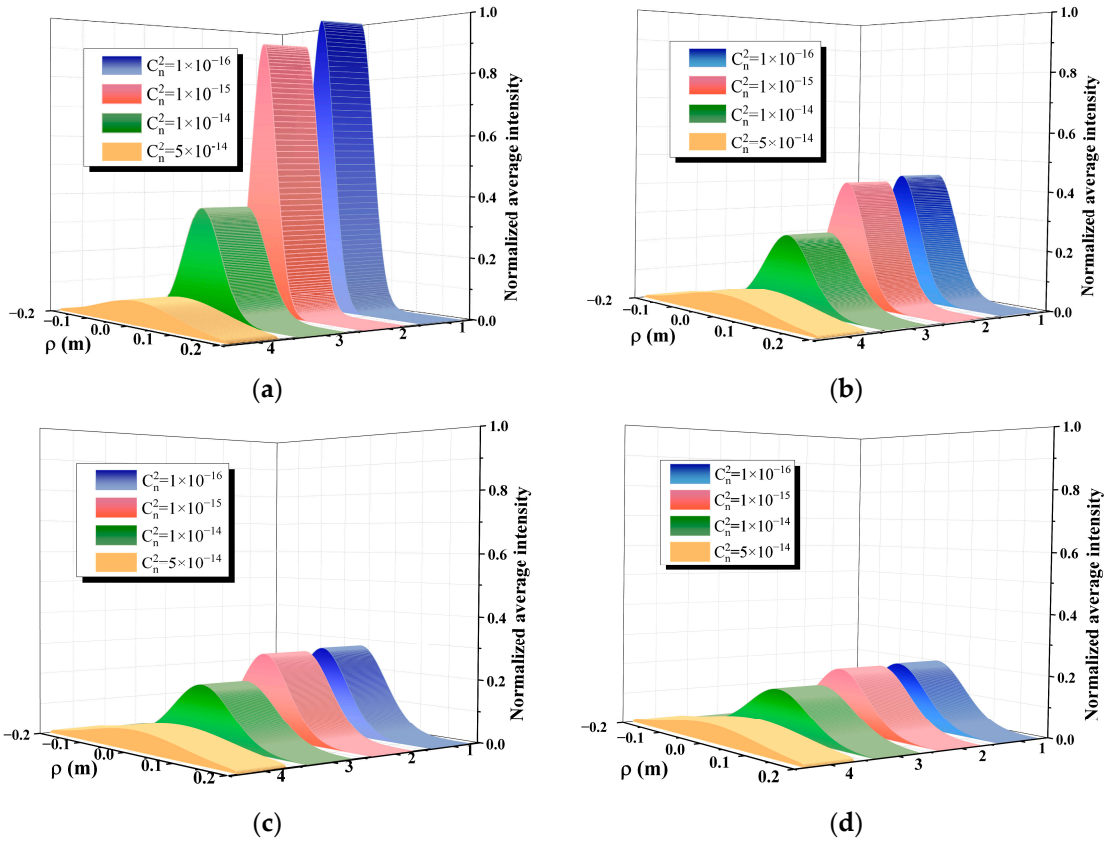

Figure 4. Normalized average intensity distributions of completely coherent light and partially coherent light at the receiving plane under different turbulence strengths. The coherence degree ℓ is (**a**) 1; (**b**) 3; (**c**) 5; (**d**) 7.

Figure 5 depicts the normalized average intensity distribution at the receiving plane for both fully and partially coherent light as a function of the transmission distance. Numerical simulations indicate that the fully coherent light exhibits a higher intensity than partially coherent light under the same transmission conditions. Additionally, as the transmission

distance increases, the beam width on the receiving plane increases for different coherence parameters of the light source, while the received light intensity decreases with distance due to the decrease in the average light intensity per unit area as the beam spreads. Interestingly, we observed a substantial decrease in the peak intensity of the average light on the receiving plane with an increase in the coherence of the light source at the same transmission distance. This is likely due to the combined effect of atmospheric turbulence and laser coherence on the received light intensity. As per the established understanding, the impact of atmospheric turbulence on the received light intensity is known to accumulate linearly with increasing transmission distance. In the case of weak turbulence conditions, the parameters of the light source dominate the received light intensity during short-distance transmission, wherein a higher coherence parameter value leads to a smaller average received light intensity. As the transmission distance increases, the effect of turbulence on light intensity increases due to the accumulation of turbulence intensity.

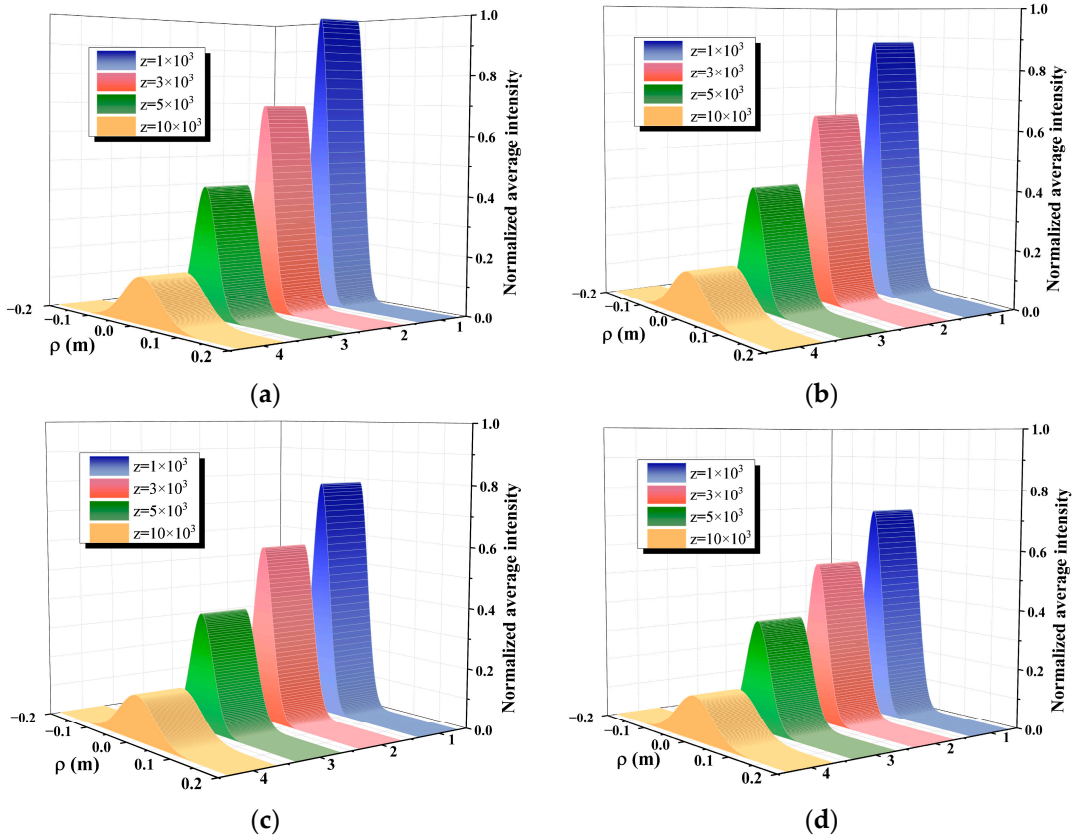

Figure 5. The normalized average light intensity distribution at the receiving plane of completely coherent light and partially coherent light at different transmission distances. The coherence degree ℓ is (**a**) 1; (**b**) 3; (**c**) 5; (**d**) 7.

3.2. The Effect of Light Source Parameters and Transmission Conditions on the Effective Beam Width and Effective Coherence Length of Partially Coherent Light Beams

The present study aims to investigate the impact of emission source parameters and turbulence intensity on effective coherence length and effective beam width during atmospheric turbulence transmission from various perspectives. Figure 6a shows that the effective beam width increases linearly with the transmission distance when the beam is transmitted in a vacuum and the source parameters are fixed. The rate of beam expansion is primarily governed by the transverse coherence length σ_h of the source field. The smaller the coherence length, the faster the beam expands and the larger the effective beam width. Figure 6b demonstrates the impact of the coherence length σ_h of the light source on the effective coherence length in a vacuum. It is shown that for short transmission distances, the

effect of the transmission distance on the effective coherence length is negligible. However, the effective coherence length increases with an increase in the coherence length of the source field. Upon long-distance transmission, the curves of different colors shown in Figure 6 converge into a single line, denoting that the coherence length is independent of source parameters and merely restricted by the increase in the transmission distance. In the presence of turbulence, Figure 6d,e reveals the alterations of the coherence length and beam width with transmission distance. Figure 6d illustrates that the beam expansion during transmission becomes more severe with the decreasing coherence of the light source. Consequently, the effective beam width no longer increases linearly with the transmission distance, as it is affected by turbulence. Furthermore, Figure 6e demonstrates that the coherence length in turbulent flow increases primarily linearly for short transmission distances. As the transmission distance increases, the coherence length decreases gradually. Upon reaching a transmission distance of 10 km, the impact of turbulent flow on the effective coherence length surpasses that of the light source parameters. From the preceding analysis, it follows that the coherence length is subject to mutual influence by both the turbulence intensity and light source parameters, with the latter influencing the extent of beam expansion. In order to eliminate the effects of beam expansion, we use the ratio of the coherence length to the beam width for our analysis. As seen in Figure 6c, during vacuum transmission, the ratio α remains constant, i.e., $\alpha = \sigma_h/\sigma_S$, irrespective of the transmission distance. This finding is consistent with the results reported in [15], which studied the vacuum transmission of GSM beams. Figure 6f presents the changes in the ratio of the coherence length to the beam width in the turbulent flow transmission. It is apparent from the figure that the ratio approaches a constant value in the case of short transmission distances, where the turbulence intensity is low; this is consistent with the behavior observed in vacuum transmissions. In contrast, the ratio decreases rapidly when the transmission distance is long, indicating the accumulation of the turbulence effect.

Figure 7 illustrates the impact of the source beam waist radius on the effective coherence length and beam width during transmission in both a vacuum and in turbulent environments. Figure 7a depicts the nearly constant behavior of the effective beam width as the transmission distance increases during vacuum transmissions over short distances. Notably, the effective beam width is positively correlated with the beam waist radius of the source field, with a larger radius resulting in a larger effective beam width. Upon increasing the transmission distance to 1 km, the effective beam width rapidly increases, and it is impervious to the light source parameters. The impact of the light source parameters on the coherence length in a vacuum is depicted in Figure 7b, where it is evident that the beam waist radius governs the rate at which the effective coherence length varies with the transmission distance. The larger the beam waist radius σ_s, the more slowly the coherence length increases. Figure 7c shows that the effective beam width's change pattern with transmission distance is analogous to that of Figure 7a when the beam is transmitted through a turbulent flow. This confirms that the light source parameters exert little influence on beam expansion in turbulent flow. Figure 7d illustrates that, for short transmission distances, the coherence length grows linearly with distance. However, for longer distances, the coherence length decreases gradually with the increase in the transmission distance. At this point, the light source parameters no longer play a dominant role in the change in the coherence length. Figure 7e shows the impact of the beam waist radius of the source beam on the ratio of the coherence length to the beam width during the propagation of the beam in turbulence. It is observed that the ratio exhibits little variation over short transmission distances, akin to the propagation in a vacuum. Notably, the ratio increases as the beam waist radius decreases, reflecting the effect of the source parameters on the beam. However, as the transmission distance increases, the impact of turbulence becomes more pronounced, leading to a decline in the ratio, which eventually approaches a steady state. This finding implies that the influence of turbulence on the beam surpasses that of the source parameters. Figure 7f presents an investigation into the effects of the source beam parameters, such as the beam waist radius and coherence length, on the ratio of coherence

length to beam width during the beam propagation in turbulent flow. The analysis reveals that for a constant ratio of beam waist radius to coherence length of the source beam, the ratio of coherence length to beam width at the same position increases with increasing values of beam waist radius and coherence length, and of their ratio in a vacuum and under turbulence.

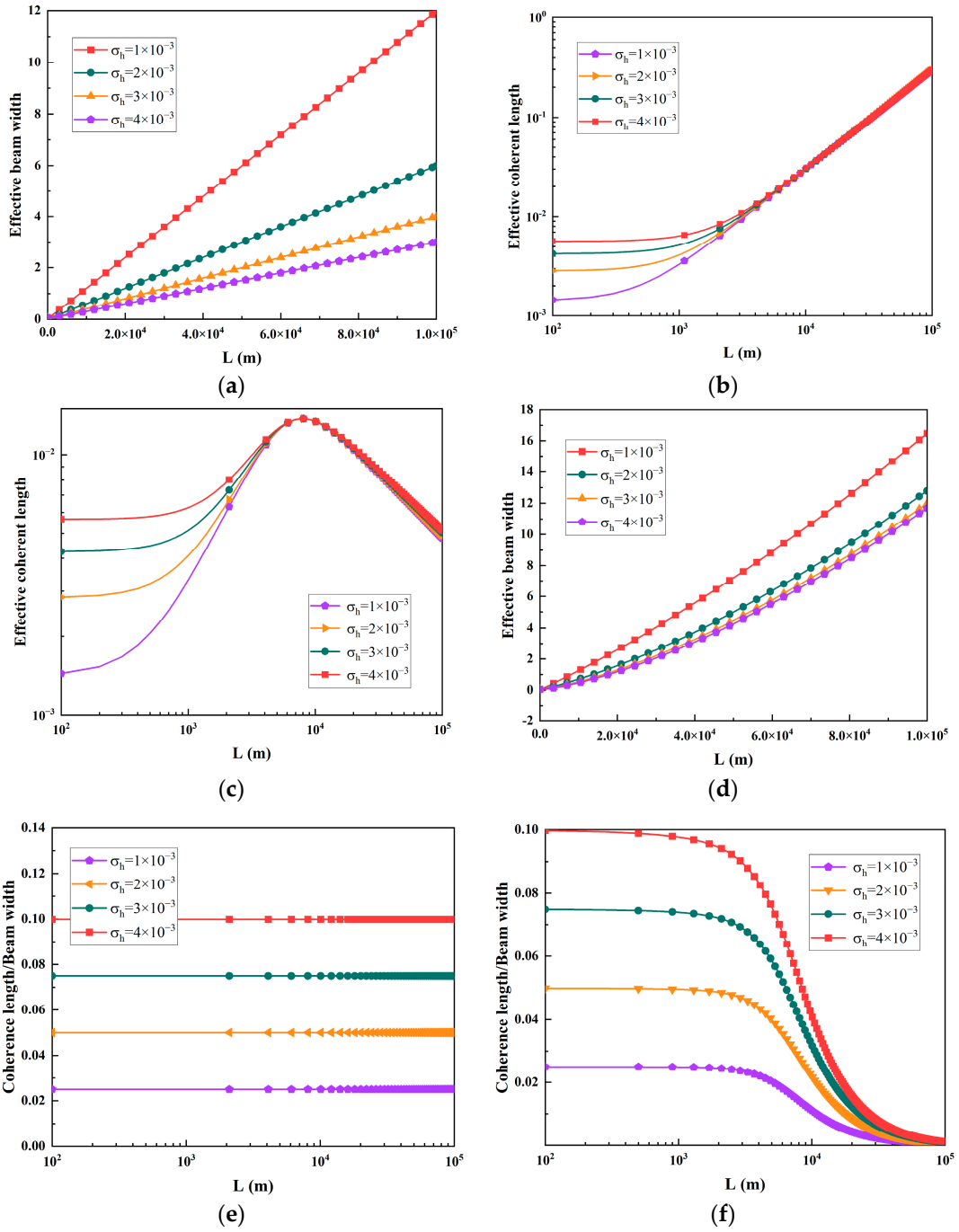

Figure 6. The influence of the coherence length of the source beam on the effective beam width, the coherence length, and their ratio in a vacuum and in turbulence. (**a**,**b**,**e**) λ = 532 nm; $l_0 = 5 \times 10^{-3}$ m; $\sigma_S = 3$ cm; (**c**,**d**,**f**) λ = 532 nm; $l_0 = 5 \times 10^{-3}$ m; $\sigma_S = 3$ cm; $C_n^2 = 10^{-15}$ m$^{-2/3}$.

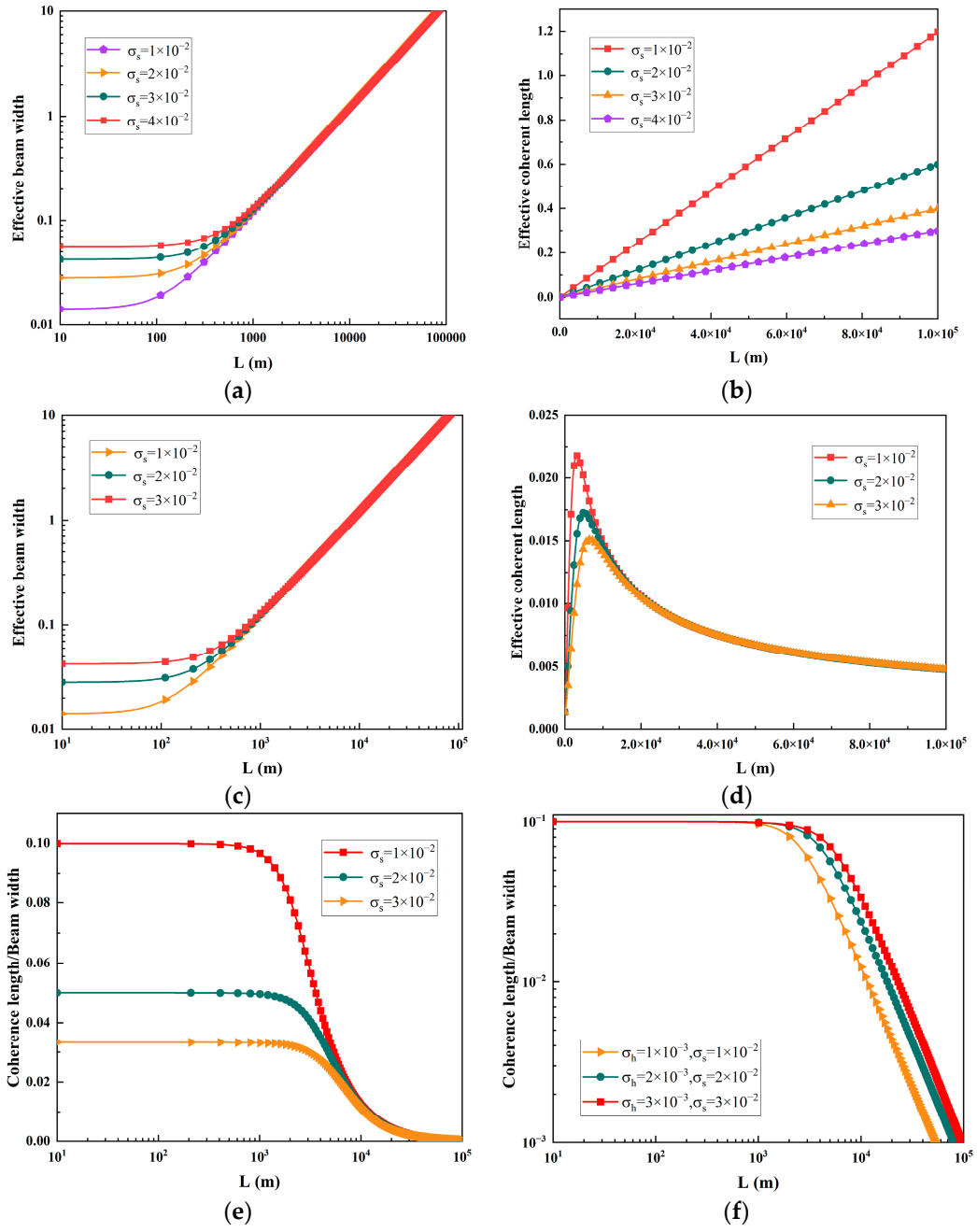

Figure 7. The influence of the beam waist radius of the source beam on the effective beam width. (**a**,**b**,**e**) λ = 532 nm; l_0 = 5 × 10^{-3} m; σ_h = 1 mm; (**c**,**d**), λ = 532 nm; l_0 = 5 × 10^{-3} m; σ_h = 1 mm; C_n^2 = 10^{-15} $m^{-2/3}$; (**f**) λ = 532 nm; l_0 = 5 × 10^{-3} m; C_n^2 = 10^{-15} $m^{-2/3}$.

Figure 8 depicts the changes in the coherence length and beam width of a beam transmitted through a turbulent flow. In particular, Figure 8a,b demonstrates the alterations in the effective beam width and effective coherence length of the received beam over varying transmission distances for distinct turbulence inner scales l_0. The results from Figure 8a reveal that the effective beam width increases with the increase in the transmission distance, resulting in the beam spreading for a fixed turbulence intensity. Furthermore, when the outer scale L_0 is kept constant, a larger inner scale l_0 corresponds to a slower growth rate of the effective beam size with the propagation distance. This behavior is explained by the fact that a smaller inner scale of turbulence results in more small eddies within the beam cross-section. Consequently, when the beam irradiates these eddies, more severe diffraction

occurs, leading to more significant beam expansion. From Figure 8b, it can be observed that the effective coherence length increases rapidly with the increasing transmission distance and then decreases slowly when the atmospheric turbulence parameters are determined. In addition, an increase in the inner scale results in a larger peak value of the effective coherence length occurring at a greater distance. Figure 8c,d depicts the changes in the effective beam width and coherence length with propagation distance under varying atmospheric refractive index structure constants. Figure 8c illustrates the evolution of the effective beam width of a beam with constant light source parameters as it propagates through a vacuum and a turbulent atmosphere. The results reveal that in the absence of turbulence, the beam width increases linearly with the propagation distance. For small values of the atmospheric refractive index structure constant, the trend is similar to that observed in a vacuum. However, as the atmospheric refractive index structure constant rises, the relationship between them does not remain linear. The effective beam width increases at a higher rate with the growth of the atmospheric refractive index structure constant. During the transmission of light beams through atmospheric turbulence, the phase distortions caused by the stochastic fluctuations in the refractive index result in beam spreading after propagating a specific distance. Figure 8d indicates that the coherence length in turbulence increases linearly with the transmission distance when the distance is relatively short, and the trend is similar to the result of transmission in vacuum. As the transmission distance increases, the coherent length decreases slowly. Figure 8e depicts the impact of the inner scale of turbulence on the coherence length to beam width ratio during beam propagation. It is observed that in the short transmission range, the ratio remains nearly constant, indicating a negligible effect of turbulence at this point. As the distance gradually increases, the smaller the inner scale, and the closer the position where the ratio decreases. With the increase in the transmission distance, the coherence length-to-beam width ratio of a propagating beam through atmospheric turbulence reduces gradually until it converges to a value of zero. Figure 8f shows that the ratio remains constant when the beam propagates through a vacuum. However, in the presence of atmospheric turbulence, the ratio decreases as the transmission distance increases. This decrease in the ratio is faster for larger values of the atmospheric refractive index structure constant.

Figure 9a–c presents the effect of wavelength on the transmission of a beam in atmospheric turbulence, showcasing the variations in the effective beam width and effective coherence length and their ratio with the propagation distance of the received beam. Figure 9a illustrates that the effective beam width increases linearly with the transmission distance, with a more pronounced increase being observed as the wavelength becomes smaller. In contrast, Figure 9b reveals that the effective coherence length of the beam increases as the wavelength decreases. Interestingly, the wavelength has a minimal effect on the ratio of coherence length to beam width, as demonstrated in Figure 9c. Further analysis of the figure reveals that smaller wavelengths allow the beam to propagate through turbulent airflow with less impact, indicating that smaller wavelengths lead to a more robust beam with a greater propagation distance.

$$\sigma_{\rho}^{2} = \frac{\iint (\boldsymbol{\rho_1} \cdot \boldsymbol{\rho_2}) I(\boldsymbol{\rho_1}) I(\boldsymbol{\rho}_2) \mathrm{d}\boldsymbol{\rho_1} \mathrm{d}\boldsymbol{\rho}_2}{\left[\int I(\boldsymbol{\rho}) \mathrm{d}\boldsymbol{\rho}\right]^2} \tag{17}$$

Equation (17) displays the drift variance σ_{ρ}^{2} of the centroid, obtained by substituting Equation (10) into Equation (17). By utilizing Figure 10, the drift variance of the beam as a function of the transmission distance L is demonstrated. The results indicate that as the transmission distance L increases, the drift variance σ_{ρ}^{2} increases gradually, and the rate of the increase in drift variance is slower in the presence of weak turbulence. Conversely, a stronger turbulence intensity leads to a faster increase in drift variance with distance. This phenomenon can be attributed to the continuous accumulation of phase disturbances generated by atmospheric turbulence, causing the drift variance of the GSM beam to increase with distance. In short distance ranges, the impact of turbulence-induced phase perturba-

tions on the beam is relatively small, leading to a smaller drift variance. However, as the distance increases, phase perturbations accumulate progressively, resulting in an increase in drift variance. This presents a common challenge in free-space optical communications, which can be partially addressed by employing adaptive optics technology or atmospheric compensation technology. Furthermore, the timescale of turbulence-induced phase perturbations also plays a crucial role in the variance of the drift, as phase perturbations with longer time scales have a more significant impact on drift variance. As turbulence intensity increases, the magnitude and time scale of the phase perturbation increase, thereby leading to a rise in the drift variance.

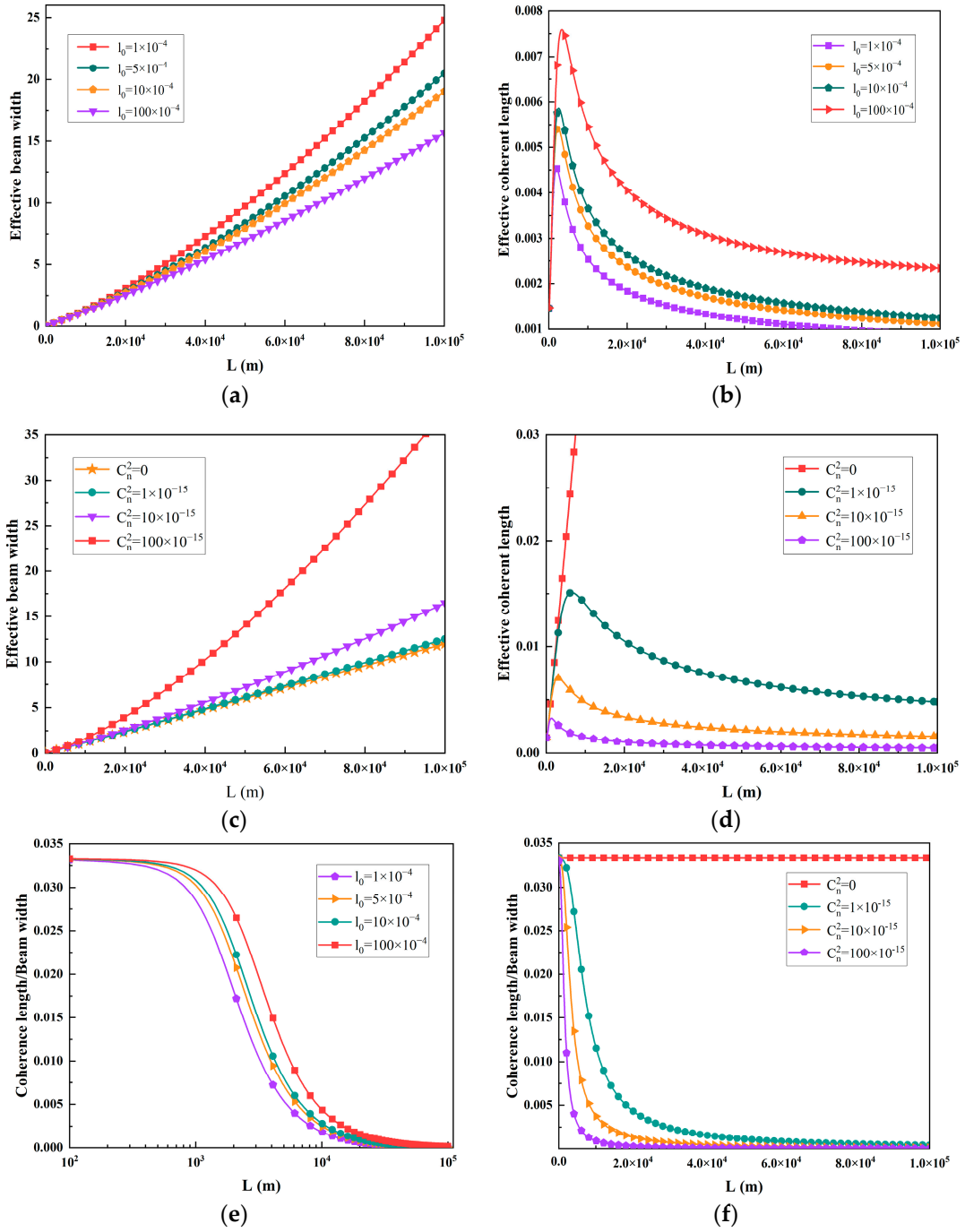

Figure 8. The impact of the atmospheric refractive index structure constant and inner scale on the beam width and coherence length and their ratio in turbulent conditions. (**a**,**b**,**e**) λ = 532 nm; σ_S = 3 cm; σ_h = 1 mm; $C_n^2 = 10^{-15}$ $m^{-2/3}$; (**c**,**d**,**f**) λ = 532 nm; σ_S = 3 cm; σ_h = 1 mm; $l_0 = 5 \times 10^{-3}$ m.

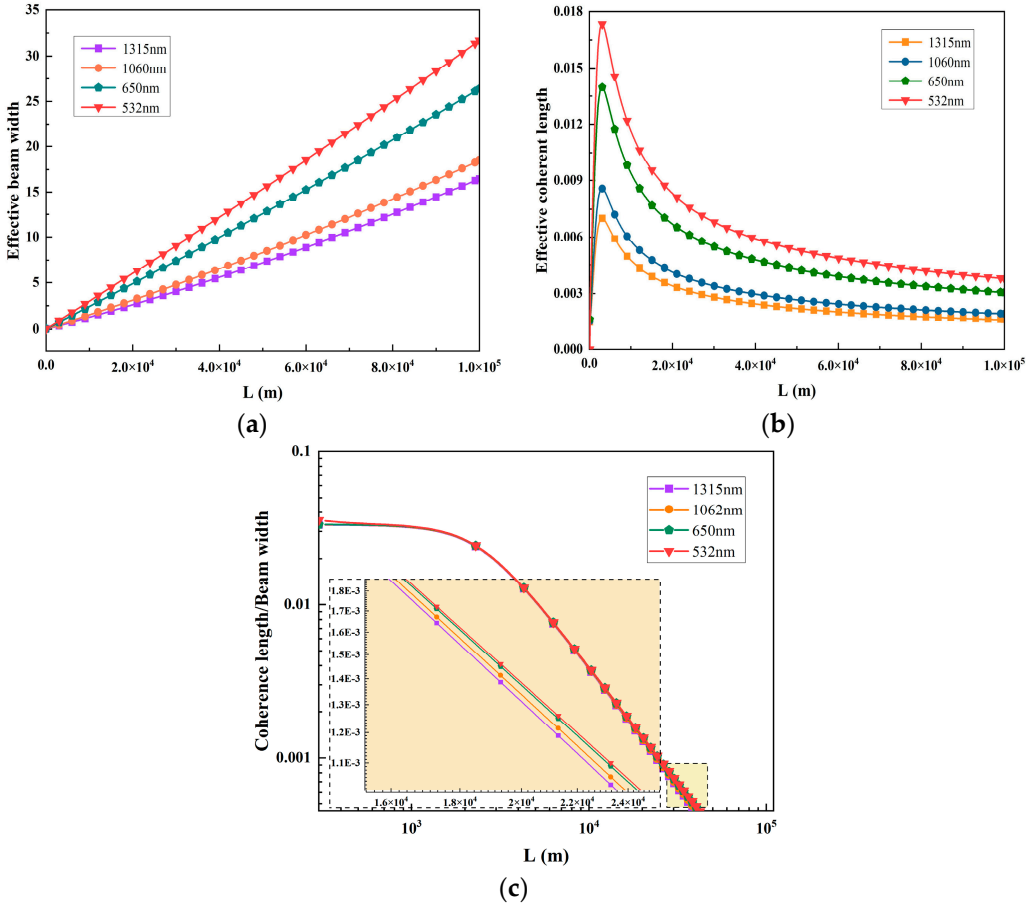

Figure 9. The impact of beam wavelength on the beam width (**a**) and coherence length (**b**) and their ratio (**c**) in turbulent conditions.

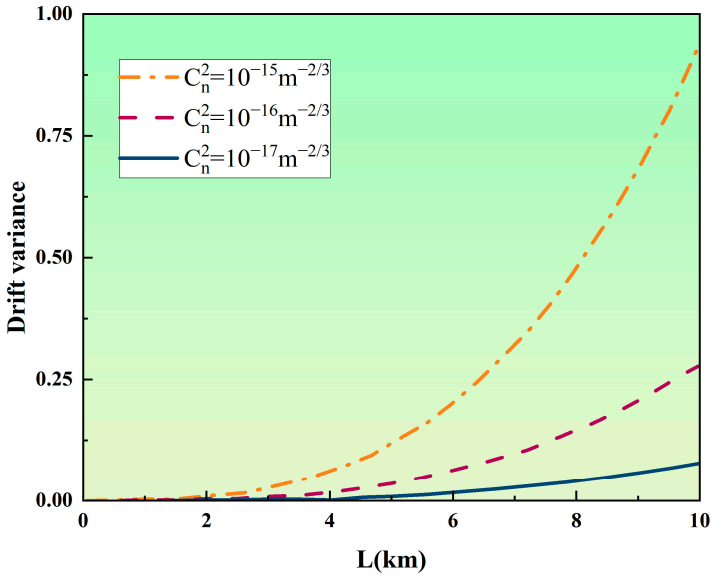

Figure 10. The impact of beam wavelength on the beam width and coherence length and their ratio in turbulent conditions.

4. Discussion

When a laser beam is transmitted through atmospheric turbulence, the wavefront of the laser is randomly perturbed, resulting in phase changes. This randomness in the wave-

front reduces the coherence of the laser wavefront, leading to a decrease in the coherence of the beam. The degree of turbulence intensity directly affects the level of randomness in the laser wavefront. Consequently, the greater the turbulence intensity, the stronger the randomness in the wavefront, leading to a weakened correlation of the original wavefront phase, and thus a lower coherence of the beam. Numerical analysis revealed that its coherence decreases due to the effect of turbulence when a beam of light is transmitted through a turbulent medium. Although the original wavefront of a partially coherent beam exhibits some degree of randomness, turbulence-induced wavefront changes are uncorrelated with the original wavefront and further diminish the spatial coherence properties of the beam. Thus, the coherence characteristics of a beam of light transmitted through atmospheric turbulence are dependent on both the source parameters and the turbulence intensity during transmission. For short transmission distances with weak turbulence, the impact of atmospheric turbulence on the beam wavefront randomness may be disregarded, whereby the coherence length is predominantly limited by the source beam's coherence parameters and waist radius. Under such circumstances, diffraction-induced beam spreading augments the coherence length. However, with an increasing transmission distance, the effect of atmospheric turbulence strengthens, resulting in a decline in the coherence length. Given that the effect of turbulence on a light beam is a cumulative process, the influence of the light source's wavefront becomes more significant with the increasing turbulence intensity, leading to a smaller peak distance for the coherence length and a faster rate of decline. With the increasing use and advancement of underwater wireless optical communications and marine remote sensing imaging applications, there has been a growing interest in the study of the beam coherence, polarization states, effective beam width, and average intensity of laser beams that propagate through turbulent ocean environments. Unlike atmospheric turbulence, ocean turbulence is affected not only by temperature changes but also by salinity fluctuations. Thus, this paper provides a comprehensive analysis of the propagation characteristics of partially coherent beams under atmospheric turbulence, which can serve as a basis for conducting more complex studies of the propagation characteristics of OAHGSM eddy beams in turbulent ocean environments in the future.

5. Conclusions

Based on the generalized Huygens–Fresnel principle, an analytical expression of the cross-spectral density function of a partially coherent beam was derived for horizontal transmission near the ground. The derived expression enabled the numerical analysis of the normalized intensity distribution and beam characteristics during atmospheric propagation. The simulation investigated the effective beam width and coherence length of the received beam under various atmospheric turbulence strengths, source coherence parameters, transmission distances, and source parameters. By comparing the coherent length variation in a vacuum transmission, the present study found that the beam parameters have a prominent influence on the coherent length variation in vacuum transmissions. The expansion of the beam leads to an increase in the coherence length, which is the outcome of the beam's free diffraction in free space. The research findings reveal that the coherence parameter of the light source and atmospheric turbulence jointly affect the effective beam width and coherence length during horizontal atmospheric transmission. During short-distance transmission, the impact of atmospheric turbulence is minimal, and the beam's transmission properties are akin to those of vacuum transmissions, with diffraction-induced beam expansion being the main factor influencing the beam's coherence length. However, during long-distance atmospheric transmissions, the superposition effect of atmospheric turbulence takes precedence, causing the coherence length to decrease. In order to exclude the influence of beam propagation, the ratio of coherent length to beam width was used for the analysis. The study shows that the ratio of coherent length to beam width with different parameters decreases under the influence of atmospheric turbulence, with the decline rate being dependent on both the beam parameters and the turbulence intensity. The analysis provides valuable insights into the intensity distribution and coherence characteristics of

beam transmission in horizontal atmospheric conditions. These findings have practical implications not only for laser transmission but also for the broader field of electromagnetic beam transmission, offering a new perspective for improving transmission efficiency. Drawing from the aforementioned findings, we present a set of tentative next steps for future research. These suggested steps encompass, but are not limited to, examining additional variables that may influence the atmospheric transmission performance of GSM beams, as well as exploring alternative hypotheses. In addition, it is recommended that forthcoming studies employ a longitudinal design, involving, for instance, beam replacement, altered turbulence conditions, and off-axis GSM beam selection, to gauge the potential long-term impacts of diverse light sources. Anticipated to be a fundamental contribution to the field, the forthcoming research will extend our understanding of laser heterodyne detection technology and its practical implications. The proposed study will focus on investigating the impact of atmospheric turbulence and scintillation on the effective beam width, pointing error, and coherence length, with respect to different atmospheric refractive index structure constants. We will conduct this analysis under various turbulence conditions, ranging from weak to strong turbulence. It is anticipated that this research will advance our knowledge of the behavior of light beams in atmospheric turbulence and provide insights into the underlying physics. The intensity distribution of a beam in atmospheric turbulence often displays a broad spatial distribution, with the maximum intensity frequently deviating from the beam axis by a certain distance. This deviation is indicative of the beam's deviation in atmospheric turbulence. Furthermore, the propagation path of the beam is subject to turbulent disturbances, resulting in a curved path. The effective radius of curvature can be used to describe this curvature of the beam's propagation path relative to the actual beam. To enhance the practical value and comprehensiveness of our analysis, we plan to conduct a further study of the influence of these factors.

Author Contributions: Conceptualization, Z.W.; methodology, Z.W.; software, Z.W.; validation, Z.W.; formal analysis, B.S.; investigation, R.W.; data curation, C.Y.; writing—original draft preparation Z.W.; writing—review and editing, S.Y.; funding acquisition, Z.F. All authors have read and agreed to the published version of the manuscript.

Funding: This research was funded by the Natural Science Foundation of Shaanxi Province, grant number 2020JM-206, the State Key Laboratory of Laser Interaction with Matter, grant number SKLLIM2103, and 111 project, grant number B17035.

Institutional Review Board Statement: Not applicable.

Informed Consent Statement: Not applicable.

Data Availability Statement: Data are available on request due to restrictions, e.g., privacy or ethical.

Acknowledgments: The authors thank the optical sensing and measurement team of Xidian University for their help.

Conflicts of Interest: The authors declare no conflict of interest.

References

1. Yousif, B.B.; Elsayed, E.E. Performance Enhancement of an Orbital-Angular-Momentum-Multiplexed Free-Space Optical Link Under Atmospheric Turbulence Effects Using Spatial-Mode Multiplexing and Hybrid Diversity Based on Adaptive MIMO Equalization. *IEEE Access* **2019**, *7*, 84401–84412. [CrossRef]
2. Dao, W.; Liang, C.; Wang, F.; Cai, Y.; Hoenders, B.J. Effects of Anisotropic Turbulence on Propagation Characteristics of Partially Coherent Beams with Spatially Varying Coherence. *Appl. Sci.* **2018**, *8*, 2025. [CrossRef]
3. Yousif, B.B.; Elsayed, E.E.; Alzalabani, M.M. Atmospheric turbulence mitigation using spatial mode multiplexing and modified pulse position modulation in hybrid RF/FSO orbital-angular-momentum multiplexed based on MIMO wireless communications system. *Opt. Commun.* **2019**, *436*, 197–208. [CrossRef]
4. Zhang, H.; Xu, L.; Guo, Y.; Cao, J.; Liu, W.; Yang, L. Application of Adam SPGD algorithm to sensor-less adaptive optics in coherent free-space optical communication system. *Opt. Express* **2022**, *30*, 7477–7490. [CrossRef]
5. Spitz, O.; Didier, P.; Díaz-Thomas, D.A.; Baranov, A.N.; Cerutti, L.; Grillot, F. Free-Space Communication With Directly Modulated Mid-Infrared Quantum Cascade Devices. *IEEE J. Sel. Top. Quantum Electron.* **2022**, *28*, 1558–1642. [CrossRef]

6. Lu, W.; Liu, L.; Sun, J.; Yang, Q.; Zhu, Y. Change in degree of coherence of partially coherent electromagnetic beams propagating through atmospheric turbulence. *Opt. Commun.* **2007**, *271*, 1–8. [CrossRef]
7. Jono, T.; Toyoshima, M.; Takahashi, N.; Yamawaki, T.; Nakagawa, K.; Yamamoto, A. Laser tracking test under satellite micro vibrational disturbances by optics ATP system. *Proc. SPIE-Int. Soc. Opt. Eng.* **2002**, *47*, 97–104.
8. Zhou, Z.-L.; Xu, C.-A.; Xu, H.-F.; Yuan, Y.-S.; Qu, J. Propagation properties of partially coherent quasi-rectangular beams in a turbulent atmosphere. *OSA Contin.* **2021**, *4*, 1234–1246. [CrossRef]
9. Ricklin, J.C.; Davidson, F.M. Atmospheric turbulence effects on a partially coherent Gaussian beam: Implications for free-space laser communication. *Opt. Soc. Am. A Opt. Image Sci. Vis.* **2002**, *19*, 1794–1802. [CrossRef]
10. Belmonte, A. Coherent return turbulent fluctuations in ground lidar systems profiling along slant paths. *Opt. Express* **2005**, *13*, 9598–9604. [CrossRef]
11. Andrews, L.; Phillips, R. Monostatic lidar in weak-to-strong turbulence. *Waves Random Media* **2001**, *11*, 233–245. [CrossRef]
12. Li, C.-Q.; Zhang, H.-Y.; Wang, T.F.; Liu, L.-S.; Guo, J. Investigation on coherence characteristics of Gauss-Schell model beam propagation in atmospheric turbulence. *Acta Phys. Sin.* **2013**, *62*, 191–197.
13. Collett, E.; Wolf, E. Is complete spatial coherence necessary for the generation of highly directional light beams? *Opt. Lett.* **1978**, *2*, 27–29. [CrossRef] [PubMed]
14. Eyyuboglu, T.; Baykal, Y.; Cai, Y. Complex degree of coherence for partially coherent general beams in atmospheric turbulence. *J. Opt. Soc. Am. A* **2007**, *24*, 2891–2902. [CrossRef] [PubMed]
15. Ricklin, C.; Davidson, F. Atmospheric optical communication with a Gaussian Schell beam. *J. Opt. Soc. Am.* **2003**, *20*, 856–866. [CrossRef] [PubMed]
16. Gbur, G.; Wolf, E. Spreading of partially coherent beams in random media. *J. Opt. Soc. Am. A* **2002**, *19*, 1592–1598. [CrossRef]
17. Xiang, N.; Wu, Z.; Hua, X.; Wang, M. Statistical properties of Gaussian -Schell beam from diffuse target in turbulent atmosphere. *High Power Laser Part. Beams* **2014**, *26*, 021003. [CrossRef]
18. Friberg, T.; Sudol, J. Propagation parameters of Gaussian Schell-model beams. *Opt. Commun.* **1982**, *41*, 383–387. [CrossRef]
19. Sahin, S.; Korotkova, O. Light sources generating far fields with tunable flat profiles. *Opt. Lett.* **2012**, *37*, 2970–2975. [CrossRef]
20. Korotkova, O.; Sahin, S.; Shchepakina, E. Multi-Gaussian Schell-model beams. *J. Opt. Soc. Am. A.* **2012**, *29*, 2159–2464. [CrossRef]
21. Ren, J.; Sun, H.; Zhao, Y.; Zhang, L. Distribution and Coherence Characteristics of PartiallyCoherent Light in Horzontal Atmospheric Propagation. *J. Atmos. Environ. Opt.* **2020**, *15*, 262–268.
22. Chang, Y.; Liu, Z.; Ni, X.; Yao, H.; Gao, S.; Gao, S.; Tong, X. Performance analysis of an all-optical double-hop free-space optical communication system considering fiber coupling. *Appl. Opt.* **2021**, *60*, 5629–5637. [CrossRef] [PubMed]
23. Liu, Y.; Liu, Z.; Chang, Y.; Liu, Y.; Jiang, H. Laboratory Measurements of the Influence of Turbulence Intensity on the Instantaneous-Fading Reciprocity of Bidirectional Atmospheric Laser Propagation Link. *Appl. Sci.* **2021**, *11*, 3499. [CrossRef]